Biomimetic Reagents for Selective Free Radical and Acid–Base Chemistry of Glycans: Application to Glycan Structure Determination by Mass Spectrometry.

4 AUTHORS, INCLUDING:

Jinshan Gao
Montclair State University
6 PUBLICATIONS **32** CITATIONS

SEE PROFILE

Chang Ho Sohn
California Institute of Technology
**11** PUBLICATIONS **117** CITATIONS

SEE PROFILE

Biomimetic Reagents for the Selective Free Radical and Acid−Base Chemistry of Glycans: Application to Glycan Structure Determination by Mass Spectrometry

Jinshan Gao, Daniel A. Thomas, Chang Ho Sohn, and J. L. Beauchamp*

Arthur Amos Noyes Laboratory of Chemical Physics, California Institute of Technology, Pasadena, California 91125, United States

Ⓢ *Supporting Information*

ABSTRACT: Nature excels at breaking down glycans into their components, typically via enzymatic acid−base catalysis to achieve selective cleavage of the glycosidic bond. Noting the importance of proton transfer in the active site of many of these enzymes, we describe a sequestered proton reagent for acid-catalyzed glycan sequencing (PRAGS) that derivatizes the reducing terminus of glycans with a pyridine moiety possessing moderate proton affinity. Gas-phase collisional activation of PRAGS-derivatized glycans predominately generates C1−O glycosidic bond cleavages retaining the charge on the reducing

terminus. The resulting systematic PRAGS-directed deconstruction of the glycan can be analyzed to extract glycan composition and sequence. Glycans are also highly susceptible to dissociation by free radicals, mainly reactive oxygen species, which inspired our development of a free radical activated glycan sequencing (FRAGS) reagent, which combines a free radical precursor with a pyridine moiety that can be coupled to the reducing terminus of target glycans. Collisional activation of FRAGS-derivatized glycans generates a free radical that reacts to yield abundant cross-ring cleavages, glycosidic bond cleavages, and combinations of these types of cleavages with retention of charge at the reducing terminus. Branched sites are identified with the FRAGS reagent by the specific fragmentation patterns that are observed only at these locations. Mechanisms of dissociation as well as application of the reagents for both linear and highly branched glycan structure analysis are investigated and discussed. The approach developed here for glycan structure analysis offers unique advantages compared to earlier studies employing mass spectrometry for this purpose.
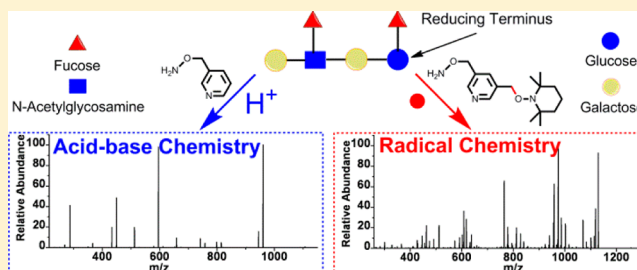
■ INTRODUCTION

Glycans make up one of the four families of structurally related macromolecules that comprise living organisms, along with nucleic acids, proteins, and lipids. However, unlike DNA, RNA, and proteins, which possess predominately linear structure comprising a limited number of subunits with defined stereochemistry, glycans may exhibit incredibly complicated branched structures with a large number of subunits having both structural and stereochemical diversity. As a result, the field of glycomics is much less developed than its siblings, genomics and proteomics. Nevertheless, genetic and biochemical studies over the past several decades have established the importance of glycans in many fields, including various aspects of health,[1] such as immunity response,[2] inflammation signaling,[3] and disease prevention,[4] as well as green energy production[5,6] and materials fabrication.[7] Therefore, understanding the structure and function of glycans will complement and strengthen other areas of research. However, complete structural characterization requires information regarding linkage, sequence, branching, and anomeric configuration. Moreover, glycans often appear in nature as a bioconjugate, with N-linked and O-linked glycoproteins being important examples. Structural characterization of glycoconjugates offers an even greater challenge.

High-performance liquid chromatography (HPLC) and electrophoresis have been widely used for glycan separation and preliminary identification. Nuclear magnetic resonance (NMR) has been used to determine the structure of glycans, especially the anomeric configuration of saccharide linkages.[8] However, this method requires milligram quantities of a highly pure sample, and interpretation of NMR spectra is relatively difficult because of the similar chemical environments of many protons.

Mass spectrometry, noted for its minimal sample consumption, high sensitivity, and short acquisition time, has been widely employed for structural characterization of glycans. Moreover, mass spectrometers allowing for tandem mass spectrometry (MS^n) have been used extensively as indispensable tools for glycan structural analysis. Ionization efficiency is especially important for the MS^n experiments to achieve good sensitivity and wide dynamic ranges. However, because of a lack of strongly basic sites for protonation, glycans are traditionally difficult to ionize. Several methods have been employed to improve sample ionization and detection, including perme-

thylation, peracetylation, and derivatization at the reducing terminus of the glycan.[9,10]

Using suitably ionized glycans, many techniques for effecting dissociation processes that provide structural information exist. Low-energy collision-induced dissociation (CID) typically generates glycosidic bond cleavage when applied to glycans.[11,12] Infrared multiphoton dissociation (IRMPD), another slow-heating fragmentation method, gives results similar to those of low-energy CID.[12,13] High-energy CID[14] and vacuum ultraviolet multiphoton dissociation[15] are unavailable on many modern instruments, even though they can generate more cross-ring cleavages than low-energy CID and IRMPD. More recently, ExD techniques, including electron capture dissociation (ECD),[12,16,17] electron detachment dissociation (EDD),[12,18,19] and electron transfer dissociation (ETD),[20,21] have been demonstrated to provide extensive and complementary information about glycan structure. Several groups have demonstrated the application of ECD in the positive ion mode for characterization of glycans with weakly basic sites,[12,16,17] while EDD has been utilized in the negative ion mode for analysis of acidic glycosaminoglycans (GAGs) by Amster and co-workers and for analysis of neutral, sialylated, and chloride-adducted glycans by Håkansson and co-workers.[12,19,20] Similarly, ETD was used to characterize a series of permethylated milk glycans in positive mode by Costello et al. and to characterize GAGs in negative mode by Amster and co-workers.[20,21] Mechanisms for ExD methods have been proposed, all of which involve radical-driven fragmentation processes accompanied by complex hydrogen migration and rearrangement.[17,18,21] Cross-ring cleavages as well as glycosidic bond cleavages were reported as the dominant fragmentation pathways. With most ExD methods, the fragmentation efficiency is often relatively low and cross-ring cleavages are not systematic and predictable because of the absence of well-defined sites of radical generation. In the EDD study of GAGs by Amster and co-workers, a nascent oxygen-centered radical is generated at a negative charge site, which in turn reacts to induce cross-ring fragmentation.[18]

Recently, several groups have employed ion mobility separations with mass spectrometry (IMS-MS) for characterization of simple isomeric oligosaccharides, the multidimensional separation of glycan mixtures, and the profiling of glycans.[22–24] However, well-characterized standards or proposed structures are needed for this technique, and the proposed structure must be verified by extensive modeling calculations.[25]

In contrast to the often unpredictable dissociation pathways and yields associated with the techniques mentioned above, natural enzymes excel in depolymerizing glycans into their components, often in a systematic and predictable manner, by taking advantage of acid–base catalysis to achieve selective cleavage of the glycosidic bond. In fact, enzymatic structural analysis of glycans employing a set of highly specific exoglycosidases, sequentially or in a matrix array, has proven to be a powerful analytical tool for the determination of sequence, linkage type, and anomeric configuration.[26] However, this method requires highly pure samples, fully completed hydrolysis, and lengthy enzymatic incubation periods. In addition, certain glycosidic bonds, particularly those between two glucose residues, are highly resistant to enzymatic degradation because of their high stability.[27] The efficiency of these natural enzymes provides impetus to develop biomimetic reagents that, when combined with MS, attempt in part to

replicate their chemistry while eliminating the shortcomings of a purely enzymatic approach to glycan sequencing.

Glycans are also highly susceptible to depolymerization by free radical processes, and their breakdown by interaction with reactive oxygen species (ROS) or reactive nitrogen species (RNS) has been extensively documented.[28] Both ROS and RNS can be generated from either exogenous or endogenous sources.[29] These two species can be either beneficial by taking part in signal transduction pathways and transcriptional regulation or detrimental by damaging lipids, glycans, proteins, RNA, and DNA.[30,31] Therefore, a biomimetic approach with synthetic reagents that utilize free radical chemistry represents a novel method for both understanding the reactions of free radicals with glycans and providing information relating to the structure of glycans.
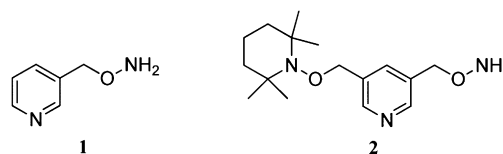

To mimic the highly selective cleavage and the importance of acid–base chemistry at the active site of natural enzymes during the process of enzymatic glycan depolymerization, we describe a sequestered proton reagent **1** for acid-catalyzed glycan sequencing (PRAGS) that derivatizes the reducing terminus of glycans with a pyridine moiety possessing moderate proton affinity. The susceptibility of glycans to dissociation by free radicals inspired us to develop a free radical-activated glycan sequencing (FRAGS) reagent **2**, which contains a free radical precursor with a pyridine moiety that can be coupled to the reducing terminus of target glycans. The FRAGS reagent was developed in analogy with the previously described technique of free radical-initiated peptide sequencing (FRIPS), in which a free radical initiator is covalently coupled to a peptide.[32–36] The FRAGS and PRAGS reagents react selectively with aldehyde and keto groups and thus target glycans with regiospecific derivatization at the reducing terminus (Scheme S1 of the Supporting Information). We demonstrate with a range of glycans that these reagents lead to systematic and predictable cleavage processes, yielding a wealth of structural information, including details of the sequence, linkage, and branching of each saccharide in the glycan.

■ EXPERIMENTAL SECTION

Materials. Glycans were purchased from Sigma-Aldrich (St. Louis, MO). All solvents are HPLC grade and were purchased from EMD Merck (Gibbstown, NJ). All other chemicals were purchased from Sigma-Aldrich. For desalting, OMIX 100 μL size C18 tips were purchased from Varian Inc. (Palo Alto, CA).

Synthesis of FRAGS and PRAGS Reagents. The synthesis strategy for the FRAGS reagent (**2**) is summarized in Scheme 1. Briefly, the FRAGS reagent synthesis was accomplished by benzylic bromination with NBS, coupling with TEMPO, reduction of the ester group, activation of the hydroxyl group, and finally hydrazinolysis of the imide group. A similar synthesis strategy excluding TEMPO derivatization was employed to synthesize the PRAGS reagent [**1** (Scheme S2 of the Supporting Information)]. For glycan derivatization, 2 μL of a 20 mM solution of the final product (**1** or **2**) in acetonitrile (ACN) was mixed with 10 μL of a 1 mM solution of the glycan in H$_2$O with 1% acetic acid (pH ~4.6). The reaction mixture was allowed to react at 60 °C for 5 h. After being desalted with C18 pipet tips according to the reported protocol,[37] the resulting glycan conjugates were ionized by electrospray ionization (ESI) coupled with

Scheme 1
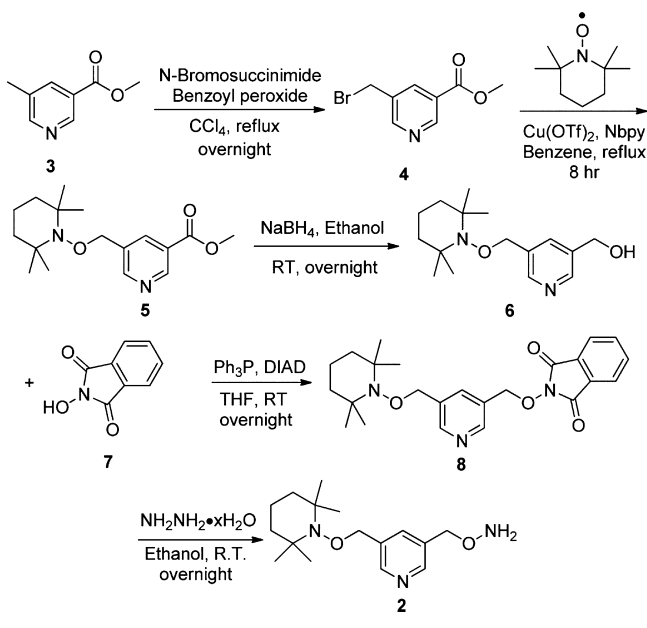
an ion trap mass spectrometer (Figure S1 of the Supporting Information). See the Supporting Information for details of the synthesis of the FRAGS reagent and glycan conjugation.

Mass Spectrometry. A Thermo-Fisher Scientific linear quadrupole ion trap (LTQ-XL) mass spectrometer (Thermo, San Jose, CA) equipped with an electrospray ionization (ESI) source was employed in experiments with both PRAGS and FRAGS. Derivatized glycan sample solutions were directly infused into the ESI source of the mass spectrometer via a syringe pump at a flow rate of 3 μL/min. Critical parameters of the mass spectrometer include a spray voltage of 5−6 kV, a capillary voltage of 30−40 V, a capillary temperature of 275 °C, a sheath gas (N_2) flow rate of 8−10 (arbitrary units), and a tube lens voltage of 50−200 V. Other ion optic parameters were optimized by the autotune function in the LTQ-XL tune program for maximizing the signal intensity. CID was performed by resonance excitation of the selected ions for 30 ms. The normalized CID energy was 7−30 (arbitrary units).

Quantum Chemical Calculation. The molecule α-1-O-methyl-D-glucopyranose was used as a simple model system to calculate key bond dissociation enthalpies (BDEs) of glycans used in this study, where BDE in this work refers to the bond dissociation enthalpy at 298 K. Initial geometries of the monosaccharide were generated by the MC/MM conformer search with the OPLS 2005 force field using Macromol 8.0 (Schrödinger Inc., Portland, OR) implemented in Maestro 8.0 (Schrödinger Inc.) in the Linux environment. Within 5 kcal/mol energy, all low-energy conformers were initially recorded. After manual screening of obtained structures to avoid redundancy, low-energy conformers were selected for further structure optimization by density functional theory (DFT). Each conformer was subject to a geometry optimization using Jaguar 7.5 (Schrödinger Inc.) at the B3LYP/6-31+G(d) level. The lowest-energy structure was then utilized as a starting point for optimization of the radical species of interest utilizing DFT at the same level of theory. The single-point energy for each species was then refined within Jaguar using B3LYP, M05-2X, and M06-2X density functionals at the 6-311++G(d,p) level of theory with the spin-unrestricted method. The two new generation *meta*-hybrid functionals other than B3LYP were chosen for their ability to more reliably predict the energetics of organic radical reactions.[38,39] Thermochemical corrections (zero-point energy and enthalpy) were obtained utilizing the B3LYP/6-311++G(d,p) level of theory and applied to all density functionals for calculation of the bond dissociation enthalpy at 298 K. All calculations were performed using computational resources kindly provided by the Material and

Process Simulation Center at the Beckman Institute of the California Institute of Technology.

BDEs were determined via the isodesmic method, in which the BDE of a reference molecule is utilized to determine the unknown BDE. To determine the BDE of C−H bonds in the monosaccharide, the enthalpy of reaction for hydrogen atom transfer between a carbon-centered methanol radical and each carbon in the sugar was calculated. The use of a reference molecule similar to the compound being studied reduces any systematic error from differences between the two species. For the determination of O−H BDEs, an oxygen-centered 2-propanol radical was utilized in place of the methanol radical. The BDEs of reference molecules were taken from the review by Blansby and Ellison.[40]

■ RESULTS AND DISCUSSION

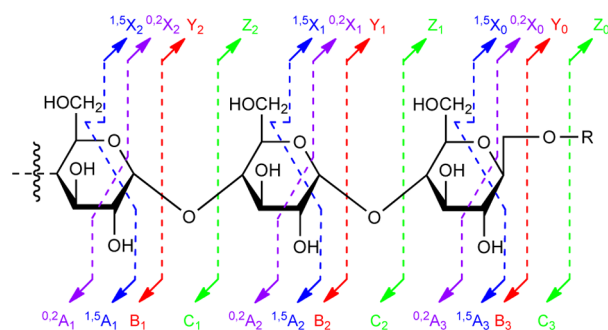All product ions are classified according to the Domon and Costello nomenclature[41] (Figure 1) except MH-TEMPO-

Figure 1. Nomenclature for glycan fragment ions.

CH_5O_2 (most likely H_2O + $HOCH_2^{\bullet}$) and Y-CH_5O_2, which were not previously reported and are defined as n ions in this study. Ions retaining the charge on the nonreducing terminus are named A (cross-ring) and B and C (glycosidic), while those ions retaining the charge on the reducing terminus are named X (cross-ring) and Y and Z (glycosidic). Letters L and H are employed to differentiate a branched glycan, where L indicates the lighter branch while H indicates the heavier branch. In displayed figures, peaks resulting from different cleavages are labeled in different colors; C1−O glycosidic bond cleavages are labeled in red, O−Cx (x can be 2, 3, 4, 5, or 6) glycosidic bond cleavages in green, 1,5-cross-ring cleavages in blue, and 0,2-cross-ring cleavages in purple.

Maltoheptaose. A simple test case for the efficacy of the glycan sequencing reagents, maltoheptaose presents a linear chain of seven identical glucose subunits (Figure 2). The gas-phase collisional activation of singly protonated PRAGS-derivatized maltoheptaose generates extensive fragmentation resulting only from C1−O glycosidic bond cleavages, retaining charge on the reducing terminus [Y ions (Figure 2)]. Except for Y_1, probabilities of glycosidic bond cleavage appear to increase with the distance from the reducing terminus of the glycan. Enzymatic glycosidic bond hydrolysis takes advantage of acid−base catalysis to achieve selective cleavage of the glycosidic bond. Here, the Y ions are proposed to form via a stepwise mechanism (Scheme 2). In the first step, the protonated pyridinium cation functions as a general acid catalyst by protonating the glycosidic oxygen. In the second step, the glycosidic bond is cleaved via the participation of the lone pair of electrons on the endocyclic oxygen to form a transition state resembling an oxocarbenium ion, with the pyridine moiety still in the proximity of the cleaved glycosidic bond. In the final
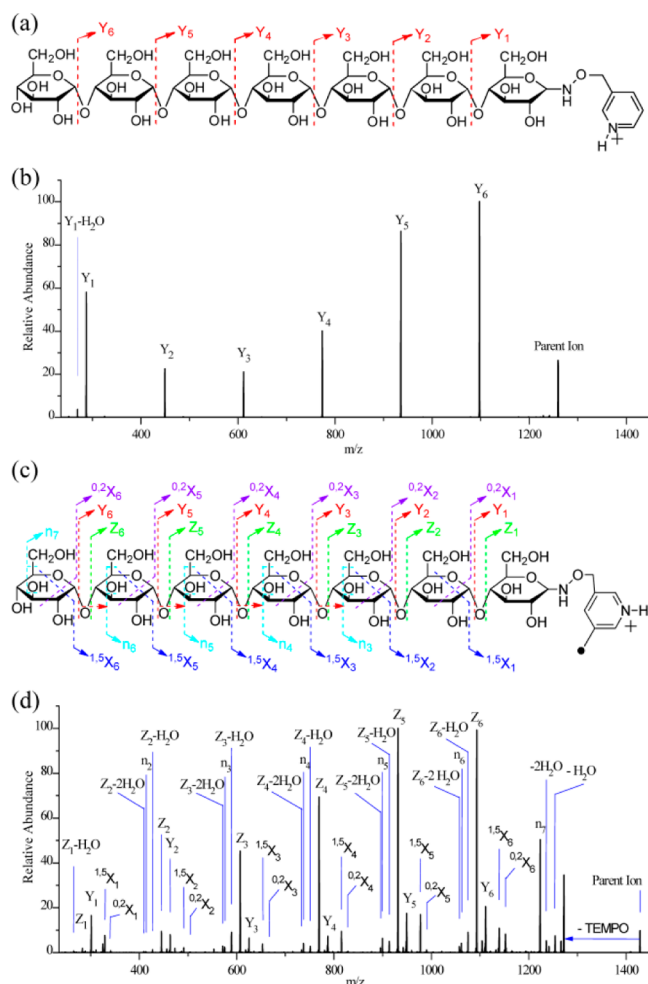
10686

dx.doi.org/10.1021/ja402810t | J. Am. Chem. Soc. 2013, 135, 10684−10692

Figure 2. Fragmentation patterns observed following CID of singly protonated PRAGS-derivatized (a) and FRAGS-derivatized (c) maltoheptaose and CID spectra of singly protonated PRAGS-derivatized (b) and FRAGS-derivatized (d) maltoheptaose. The parent ion refers to the protonated molecular ion. The possible fragmentation of the reducing terminus glycan subunit is not observed because of the low mass cutoff.

Scheme 2
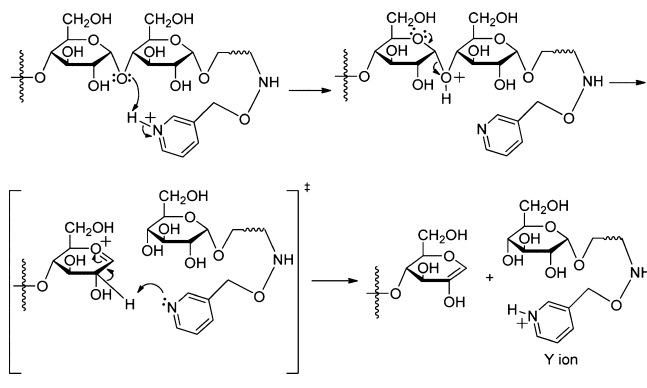
step, this pyridine moiety serves as a base to deprotonate the oxocarbenium ion to form the observed Y ion. The gas-phase proton affinities of oxygen atoms in α-D-glycopyranose are calculated to be 204−214 kcal/mol,[42] a range lower than that of pyridine, 222 kcal/mol.[43] Alternatively, association of the protonated pyridine with the glycosidic oxygen facilitates a β-

hydrogen transfer to oxygen (Scheme S3 of the Supporting Information), which is similar to the β-hydrogen transfer of protonated diethyl ether resulting in loss of ethylene during multiphoton dissociation.[44] The requirement of acid catalysis involving the labile proton is supported by CID of singly protonated maltoheptaose derivatized with Girard's T (GT) reagent, a similar aldehyde- and keto-reactive molecule with a fixed charge quaternary ammonium moiety.[45] In contrast to the protonated charge site of the PRAGS reagent, the inability of this reagent to donate a proton leads to an increase in the CID energy required for a significant extent of fragmentation, and the spectrum is dominated by loss of H_2O instead of glycosidic bond cleavage (Figure S2 of the Supporting Information). The glycosidic bond cleavage in this case is proposed to result from a concerted four-membered ring rearrangement, needing energy input to overcome the reaction barrier higher than that required for acid/base-catalyzed glycosidic cleavage (Scheme S4 of the Supporting Information).

Maltoheptaose was employed as a model for linear glycans as it has been well studied by CID, ECD, and EDD mass spectrometry.[12,17,19,46] The peak assignments are unambiguous as only Y ions are observed, providing composition and sequence information for the structural analysis of maltoheptaose. This behavior is quite different from that revealed by CID of $[M + \text{metal}]^+$,[47] $[M_{\text{permethylated}} + Na]^+$,[17] $[M − H + Cl]^{2−}$,[19] and $[M − 2H]^{2−}$[12] glycans, wherein not only Y ions but also A, B, C, X, and Z ions are observed. Because of the symmetry of maltoheptaose, multiple pairs of isobaric product ions (B and Z, C and Y, and A and X ions) make the assignment ambiguous. Differentiation of such ambiguous fragments has been achieved via reduction or ^{18}O labeling of the reducing terminus.[46]
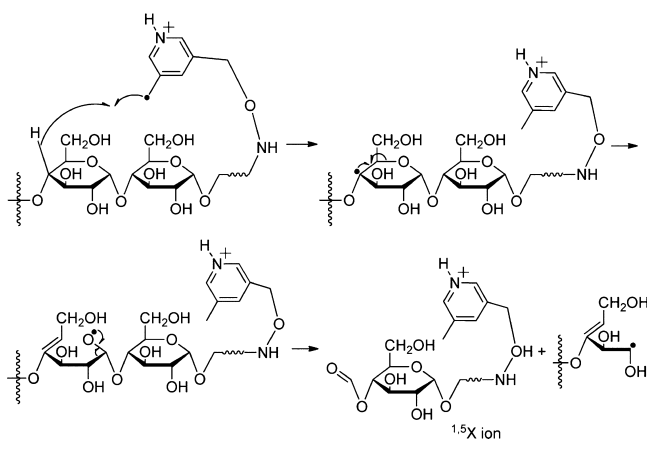
Collisional activation of singly protonated FRAGS-derivatized maltoheptaose induces not only C1−O glycosidic bond cleavage but also O−Cx glycosidic bond cleavage and cross-ring cleavages. Many more free radical-driven fragmentation pathways in the gas phase are observed compared with that observed previously in solution.[28] A series of abundant and systematic dissociation patterns, including $^{0,2}X$, $^{1,5}X$, Z, and n ions, are observed and proposed to be driven by hydrogen abstraction followed by rearrangement, as detailed in subsequent discussion. As the Z, $^{1,5}X$, $^{0,2}X$, and n ions are not observed in the CID spectrum of singly protonated PRAGS-derivatized maltoheptaose, they are proposed to occur via free radical-driven mechanisms. In the first step of Z ion formation, the nascent free radical, the carbon-centered radical formed on the FRAGS reagent, abstracts a hydrogen atom from C5 to generate a carbon-centered radical at this site. In the second step, the resulting radical promotes homolytic cleavage of the glycosidic bond via formation of a double bond between C4 and C5 (Scheme 3). An alternative mechanism involving abstraction of hydrogen from nonreducing terminus C′1−H′1 (anomeric) followed by O−C4 homolytic cleavage and loss of C5−H5 radical is also possible (Scheme S5 of the Supporting Information). Similar to the formation of Z ions, the formation of $^{1,5}X$ ions (Scheme 4), $^{0,2}X$ ions (Scheme S6 of the Supporting Information), and n ions (Scheme S7 of the Supporting Information) is initiated by hydrogen abstraction by the nascent free radical followed by β-bond cleavages.

Compared with CID of singly protonated PRAGS-derivatized maltoheptaose, CID of singly protonated FRAGS-derivatized maltoheptaose provides much more structural information (Figure 2). All the Y-type fragmentation generated

10687

dx.doi.org/10.1021/ja402810t | J. Am. Chem. Soc. 2013, 135, 10684−10692
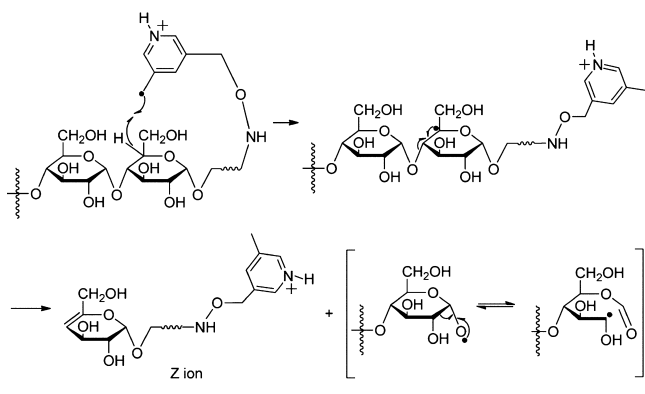
Scheme 3

Scheme 4

from CID of singly protonated PRAGS-derivatized maltohep-taose is observed in the CID spectrum of singly protonated FRAGS-derivatized maltoheptaose. The observed product ions are sufficient for the comprehensive structural analysis of maltoheptaose. Systematic glycosidic bond cleavages (Y and Z ions) provide composition and sequence information, while the cross-ring cleavages ($^{0,2}X$ and $^{1,5}X$ ions) and loss of CH_5O_2 (n ion) provide linkage information. Employing the FRAGS and PRAGS reagents, the product ions retain charge on the reducing terminus, simplifying the analysis of CID spectra. The systematic cross-ring and glycosidic bond cleavages observed with high fragmentation efficiency using the FRAGS reagent provide the expectation that unknown glycan structures can be inferred from their fragmentation patterns.

Disaccharide Isomers. To assess the ability of the PRAGS and FRAGS reagents to differentiate isobaric glycan structures, we examined the dissociation of several disaccharide isomers. Maltose is a glycan that consists of two glucoses bonded through an $\alpha 1-4$ linkage, whereas cellobiose is an isobaric glycan that consists of two glucoses bonded through a $\beta 1-4$ linkage. Lactose differs from cellobiose only in the stereo-chemistry of C4 in the nonreducing terminus glycan subunit, whereas nigerose differs from maltose and cellobiose only in the linkage type. Collisional activation of these four singly protonated PRAGS-derivatized disaccharides generates exclu-sively C1−O glycosidic bond cleavage [forming a Y ion (b, e, h, and k in Figure 3)], with no significant difference in the mass spectra of the four structural isomers. However, with the FRAGS-derivatized glycans, structures of which are shown in Figure 3, collisional activation of [M + H − TEMPO]$^+$ ions of

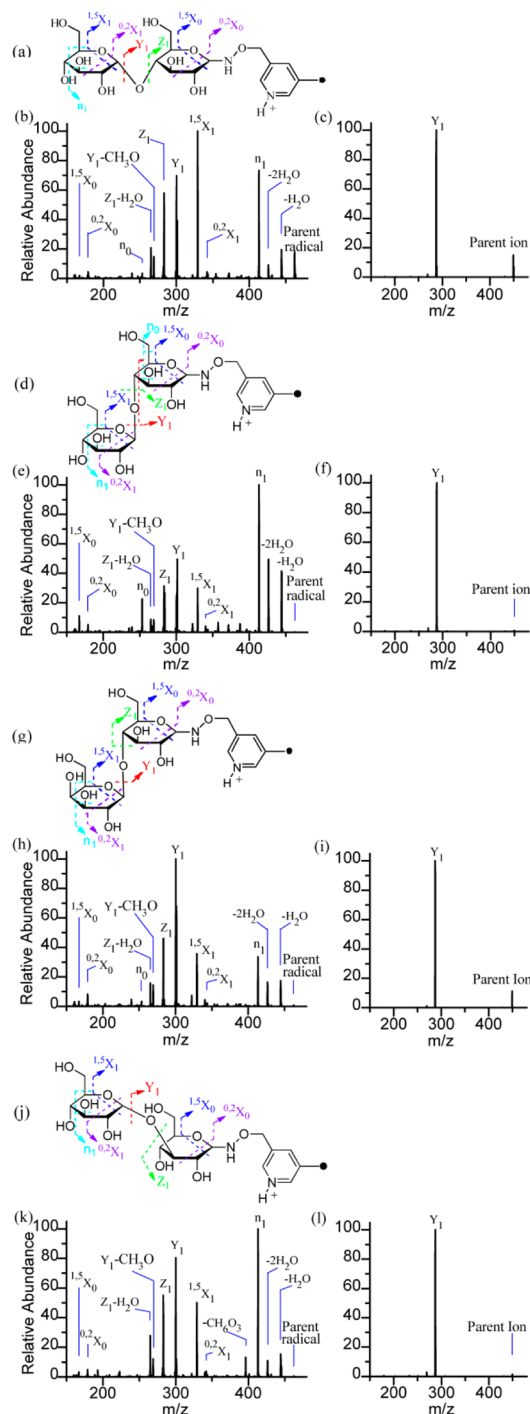**Figure 3.** CID spectra of [M + H − TEMPO]$^+$ ions of maltose (b), cellobiose (e), lactose (h), and nigerose (k), CID spectra of PRAGS-derivatized maltose (c), cellobiose (f), lactose (i), and nigerose (l), and fragmentation patterns observed following CID of [M + H − TEMPO]$^+$ ions of maltose (a), cellobiose (d), lactose (g), and nigerose (j). CID spectra c, f, i, and l are nearly identical, dominated by the Y$_1$ ion. CID spectra b, e, h, and k are different in the branching ratios of the product ions.

these four disaccharides generates more extensive fragmenta-tion (a, d, g, and j in Figure 3), including glycosidic bond cleavage (Y and Z ions), cross-ring cleavage ($^{1,5}X$ and $^{0,2}X$), and −CH_5O_2 (most likely H_2O + $HOCH_2^\bullet$) cleavage (n ion). The [M + H − TEMPO]$^+$ ions of the disaccharides are generated by CID of the corresponding singly protonated FRAGS-

derivatized glycans (Figure S3 of the Supporting Information). While the FRAGS CID spectra of the four isomers generate the same product ions, the relative intensities are significantly different. To clearly see how the FRAGS reagent differentiates the four disaccharide isomers, the branching ratios (fraction of total fragment yield) of each sugar are compared (Figure 4).
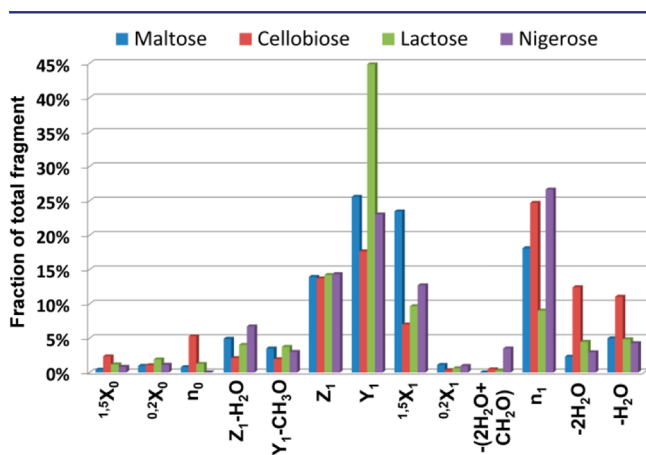

Figure 4. Branching ratios (fraction of total fragment yield) of different fragmentation patterns of the four disaccharide isomers. They mainly differ in the branching ratios of Y_1, $^{1,5}X$, $-CH_6O_3$, n_0, and n_1 ions. For each fragmentation pattern, maltose, cellobiose, lactose, and nigerose are shown from left to right, respectively.

Significant differences are observed in fragment yields of Y_1, $^{1,5}X_1$, $-CH_6O_3$ (most likely $CH_2O + 2H_2O$), n_0, and n_1. The $^{1,5}X_1$ ion is the base peak (most abundant fragment) for maltose; the n_1 ion is the base peak for cellobiose, and the Y_1 ion is the base peak for lactose. The significant decrease in the intensity of the n_1 ion for lactose is attributed to the presence of a *cis*-diol on C3 and C4, according to the general mechanism postulated for the formation of the n ion as shown in Scheme S7 of the Supporting Information. The relatively high intensity of the $^{1,5}X_1$ ion for maltose may be due to the fact that the hydrogen on C4′ (nonreducing subunit) of maltose is more accessible than in the other isomers. Although the n_1 ion is the base peak for both nigerose and cellobiose, the relative abundances of the Y_1 and $-CH_6O_3$ ions are higher for nigerose. The neutral loss of CH_6O_3 is proposed to occur via hydrogen abstraction by the nascent free radical followed by rearrangement, as shown in Scheme S8 of the Supporting Information. The relatively high intensity of the $-CH_6O_3$ ion for nigerose compared to the intensities for the other three isomers may be rationalized by the fact that the hydrogen on C1′ (nonreducing subunit) is highly accessible to the nascent free radical. Clearly, the n_0 ion of cellobiose is significantly more abundant than the other three disaccharide isomers. Overall, the difference in fragment ion abundances in the FRAGS CID spectra allows the glycan isomers to be readily distinguished.

Lacto-*N*-difucohexaose II (LNDFH II). Two complex branched glycans, Lewis-Y tetrasaccharide and LNDFH II, were also examined with the new reagents. We present here the analysis of the more complex LNDFH II, and the analysis of data for Lewis-Y tetrasaccharide is presented in the Supporting Information. LNDFH II is employed as a highly branched model glycan, having a reducing terminus in the center and a branch on the *N*-acetylglucosamine unit, to assess the ability of FRAGS and PRAGS reagents to analyze more complicated

glycan structures. Collisional activation of singly protonated PRAGS-derivatized LNDFH II (Figure 5) mainly generates not
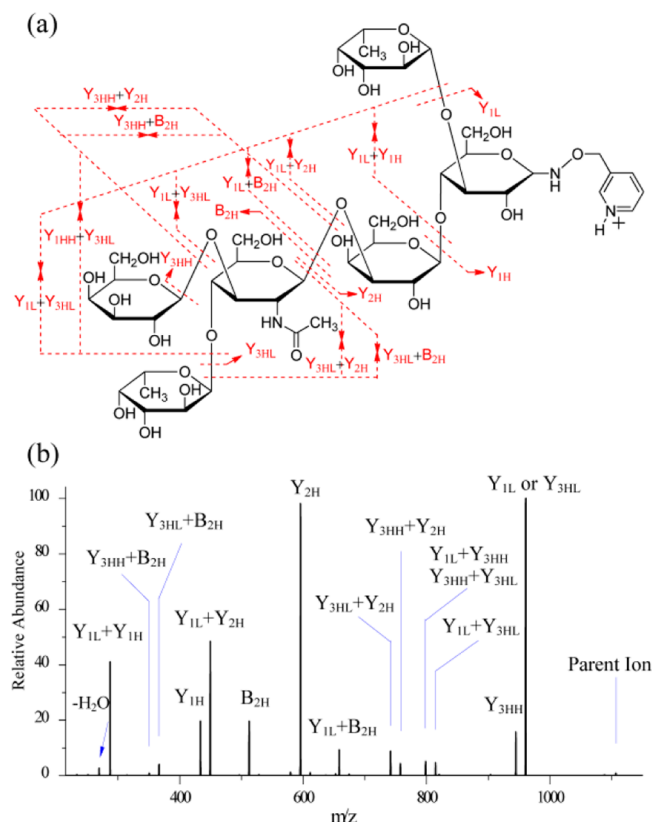

Figure 5. Fragmentation patterns observed following CID of singly protonated PRAGS-derivatized LNDFH II (a) and CID spectrum of singly protonated PRAGS-derivatized LNDFH II (b).

only systematic Y ions but also Y+Y ions. The Y+Y ions result from a pair of C1−O glycosidic bond cleavages. As with the simple glycans discussed above, the PRAGS reagent systematically deconstructs the glycan, revealing subunit connectivity. This can be illustrated in the deconstruction (DECON) diagram, which serves to visually summarize the MS^n results, shown for LNDFH II in Figure 6. The sequence, composition, and branching of LNDFH II can be discerned from this diagram. Three pairs of product ions, Y_{3HH} (*m/z* 960.6) and Y_{3HL} (*m/z* 944.6), $Y_{1L}+Y_{3HH}$ (*m/z* 814.5) and $Y_{1L}+Y_{3HL}$ (*m/z* 798.5), and $Y_{1L}+Y_{2H}$ (*m/z* 499.5) and Y_{1H} (*m/z* 433.4), can be employed to infer the existence of two branches in the glycan structure. Moreover, $Y_{1L}+Y_{2H}$ and Y_{1H} ions can be employed to elucidate the site of the reducing terminus of LNDFH II. It needs to be noted that the $Y_{3HL}+Y_{2H}$ and $Y_{3HH}+Y_{2H}$ ions result from the internal loss of *N*-acetylglucosamine, and the $Y_{1L}+B_{2H}$ ion is formed by the migration of fucose.[48,49] This may be a potential problem for the structure determination of the unknown glycans. Furthermore, the generation of B_{2H} (*m/z* 512.5), $Y_{3HL}+B_{2H}$ (*m/z* 366.3), and $Y_{3HH}+B_{2H}$ (*m/z* 350.3) ions provides information about the location of *N*-acetylated saccharide units, even though they make the spectrum more complicated. This can be rationalized by considering the proton affinity of pyridine (222 kcal/mol) and an amide (*N*-methylacetamide, 212 kcal/mol),[43] which makes it possible to protonate the *N*-acetyl group and therefore to generate B ions,
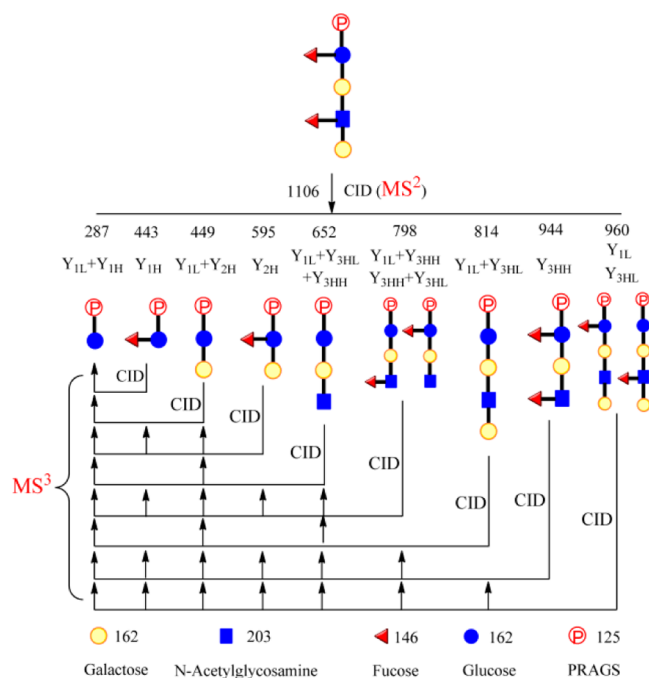
10689

dx.doi.org/10.1021/ja402810t | *J. Am. Chem. Soc.* 2013, 135, 10684−10692

Figure 6. Glycan DECON diagram for LNDFH II. The precursor ion (m/z 1106) is subjected to MS^2 to generate a series of ions with m/z values from 287 to 960. The MS^2 product ions are isolated and subjected to CID to generate MS^3 product ions indicated by upward-pointing arrows.
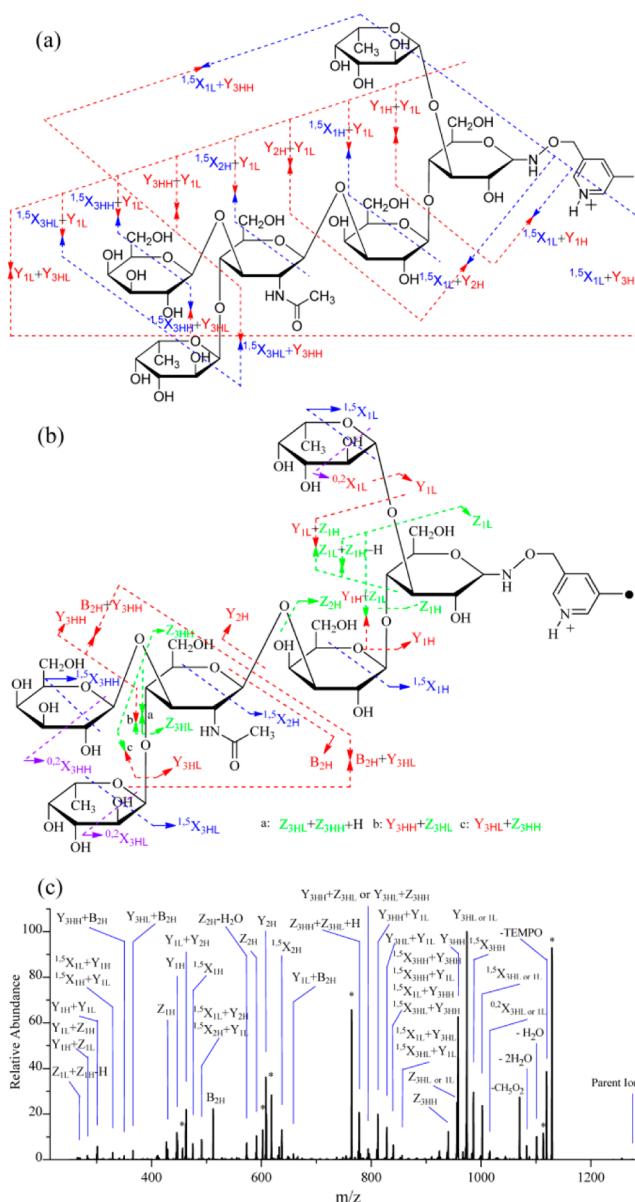

Figure 7. Fragmentation patterns observed following CID of singly protonated FRAGS-derivatized LNDFH II (a and b; two schemes are employed because there is not enough space to label all fragmentation patterns) and CID spectrum of singly protonated FRAGS-derivatized LNDFH II (c). Peaks marked with asterisks are the products ions corresponding to the glycosidic bond cleavages from the parent ion.

even though the relative abundance is low compared with that of Y ions.

All the fragmentation patterns generated via CID of singly protonated PRAGS-derivatized LNDFH II can also be found in the CID spectrum of singly protonated FRAGS-derivatized LNDFH II (Figure 7). In addition, the generation of systematic series of $Y+^{1,5}X$ ions can be employed to illustrate the existence of the two branch sites in LNDFH II. Four more characteristic ions, $Z_{1H}+Z_{1L}$-H (m/z 265.1), $Z_{1H}+Y_{1L}$ (or $Z_{1L}+Y_{1H}$, m/z 283.1), $Z_{3HH}+Z_{3HL}$+H (m/z 778.3), and $Z_{3HL}+Y_{3HH}$ (m/z 794.3), also provide direct evidence of the existence of the two branch structures. The $Z_{1H}+Z_{1L}$-H ion can be employed to infer the site of the reducing terminus. Lewis-Y tetrasaccharide has an analogous structural feature, and the location of the reducing terminus can be similarly inferred from the related fragmentation patterns (Figure S5 of the Supporting Information). A suggested mechanism for the formation of the $Z_{1H}+Z_{1L}$-H ion is presented in Scheme S9 of the Supporting Information.

The proposed mechanism of formation of the $Z_{3HH}+Z_{3HL}$+H ion is shown in Scheme 5. The nascent free radical abstracts a hydrogen atom from C1 of one of the branched glycan units. The resulting carbon-centered radical drives the cleavage of the glycosidic bond and formation of a radical on C4 of the N-acetylglucosamine unit, followed by the formation of a double bond between C3 and C4, and finally a second glycosidic bond cleavage to generate the $Z_{3HH}+Z_{3HL}$+H ion (Scheme 5). The structure of the $Z_{3HH}+Z_{3HL}$+H ion is confirmed by CID of this characteristic ion as shown in Figure S4 of the Supporting Information.

Calculations. To gain further insight into the hydrogen atom abstraction processes observed with the FRAGS reagent, C−H and O−H bond dissociation enthalpies of α-1-O-methyl-D-glucopyranose were calculated as described in the Exper-

imental Section. These are displayed graphically in Figure 8. In agreement with the proposed mechanisms and previous literature, the BDEs of O−H bonds are significantly higher than those of C−H bonds. In all cases, the C−H BDEs for the glycan fall within a narrow range and indicate a slightly endothermic reaction for hydrogen atom abstraction by the FRAGS reagent (benzyl BDE of ∼90 kcal/mol).[40] Although the BDE values calculated at the three theory levels are different, it is clear that the trends for relative energies are quite similar. A more thorough potential energy surface exploring subtleties in conformation and interaction would be necessary to compare the relative reactivities of each carbon site and estimate the activation energies, which are likely to be significantly in excess of the small 4−6 kcal/mol endothermicity. In addition, the relative abundance of product ions in FRAGS spectra induced
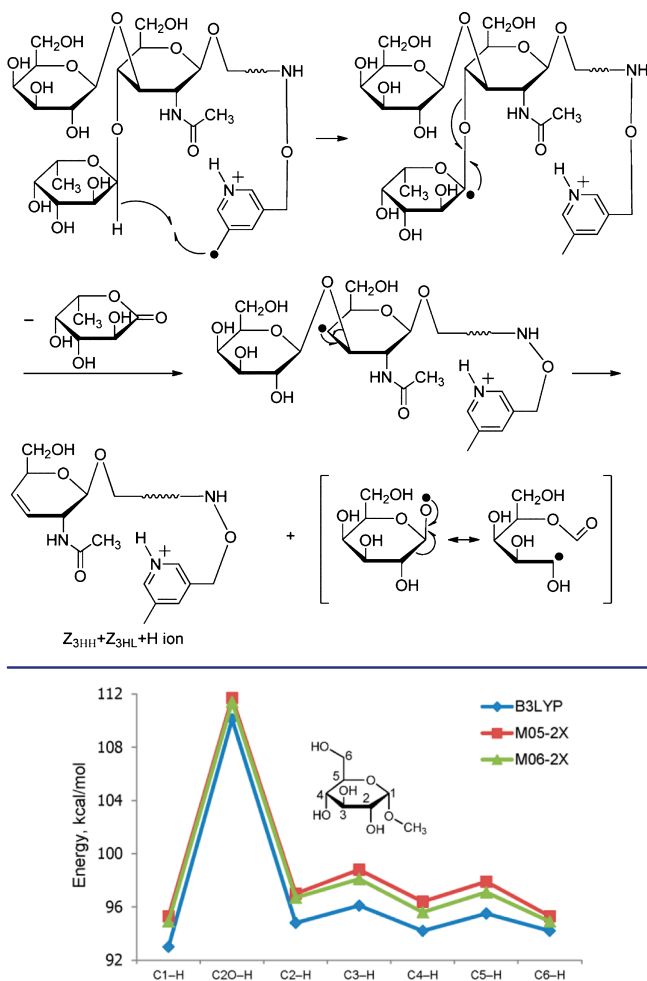
Scheme 5

Figure 8. R–X bond dissociation enthalpies (ΔH_{298}) for α-1-O-methyl-D-glucopyranose. For the M05 and M06 density functionals, the uncertainties of the calculated BDEs are estimated to be 0.5–1.0 kcal/mol according to extensive comparisons of the computational methods to relatively well-known bond dissociation enthalpies.[38]

by free radical chemistry is slightly higher than those resulting from acid–base chemistry, suggesting that the activation energies for free radical-driven processes are slightly lower than those for acid–base chemistry. However, reasonable yields of both types of product ions are generally observed.

■ CONCLUSION

The capability of two new biomimetic reagents, PRAGS and FRAGS, to determine structure of both linear and highly branched glycans, and differentiating glycan isomers, is demonstrated. It is noted that this experimental methodology requires that the glycans possess a reducing terminus. Both the PRAGS and FRAGS reagents add a pyridine moiety to the reducing terminus of the glycan, providing a site of moderate proton affinity that both enhances ionization efficiency and effects glycosidic bond cleavage. Similar to enzymatic glycosidic bond cleavage, PRAGS employs acid–base chemistry to effect selective C1–O glycosidic bond cleavage (Y ions), with the charge retained on the reducing terminus. The resulting systematic PRAGS-directed deconstruction of the glycan inspired the development of a glycan diagrammatic approach (DECON diagram), which allows the assembly of the glycan

skeleton. The results of MS^n studies are incorporated in the diagram and serve to further confirm the assigned structure. With both a labile proton and radical precursor, collisional activation of FRAGS-derivatized glycans yields abundant cross-ring as well as glycosidic bond cleavages, resulting from both free radical and acid–base chemistry, with retention of charge at the reducing terminus. Branched sites are readily identified with the FRAGS reagent as a result of specific fragmentation processes that result from free radical chemistry.

Unlike the consistent linear arrangement of subunits connected by amide bonds in the case of proteins and phosphodiester bonds in the case of oligonucleotides, the variability in glycan linkages renders the determination of oligosaccharide structure especially challenging. This complexity is evident even for relatively simple isobaric disaccharides, as shown in Figures 3 and 4. Given that each of the four molecules exhibits significant differences in product ion intensities, the use of mass spectrometry-based database searching for the identification of unknown glycans from a library of reference spectra would permit identification of structural isomers. However, it is not possible at present to relate the data shown in Figure 3 to distinct disaccharide structures without additional information. Nevertheless, the results for the analysis of the highly branched hexasaccharide LNDFH II employing the PRAGS and FRAGS reagents reveal the utility of these reagents for unraveling many of the structural features of highly branched glycans. In addition, the generation of B and B+Y ions upon CID of singly protonated LNDFH II can be employed to indicate the existence and substitution site of an N-acetylated glycan unit.

The high CID fragmentation efficiency and quantitative conversion of glycan to bioconjugates (Scheme S1 of the Supporting Information) employing these reagents facilitate their application in addressing problems in structural glycobiology. The systematic fragmentation patterns obtained upon dissociation lend themselves to interpretation using bioinformatic approaches. The range of glycan structures comprising the model linear and branched glycans considered in this study is representative of the major glycan subunits commonly encountered in vertebrate biology. Future studies will consider a wider range of glycan subunits, substituent groups, and branching patterns. Finally, the success in determining glycan structures employing PRAGS and FRAGS suggests that the reagents for free radical-initiated peptide sequencing (FRIPS)[32] developed earlier in our laboratory will also find application in the structural analysis of glycoproteins, the most important family of glycoconjugates. Preliminary results support the feasibility of this approach.

■ ASSOCIATED CONTENT

ⓢ Supporting Information

Proposed mechanisms of ion fragmentation, discussion of Lewis-Y tetrasaccharide, experimental procedures, and ^{1}H and ^{13}C NMR spectra. This material is available free of charge via the Internet at http://pubs.acs.org.

■ AUTHOR INFORMATION

Corresponding Author
jlbchamp@caltech.edu

Notes
The authors declare no competing financial interest.

◼ REFERENCES

(1) Varki, A.; Etzler, M. E.; Cummings, R. D.; Esko, J. D. In *Essentials of Glycobiology*, 2nd ed.; Varki, A., Cummings, R. D., Esko, J. D., Freeze, H. H., Stanley, P., Bertozzi, C. R., Hart, G. W., Etzler, M. E., Eds.; Cold Spring Harbor Laboratory Press: Plainview, NY, 2009.

(2) Rabinovich, G. A.; Toscano, M. A. *Nat. Rev. Immunol.* **2009**, *9*, 338−352.

(3) Sorokin, L. *Nat. Rev. Immunol.* **2010**, *10*, 712−723.

(4) Walker, L. M.; Sok, D.; Nishimura, Y.; Donau, O.; Sadjadpour, R.; Gautam, R.; Shingai, M.; Pejchal, R.; Ramos, A.; Simek, M. D.; Geng, Y.; Wilson, I. A.; Poignard, P.; Martin, M. A.; Burton, D. R. *Proc. Natl. Acad. Sci. U.S.A.* **2011**, *108*, 20125−20129.

(5) Himmel, M. E.; Ding, S. Y.; Johnson, D. K.; Adney, W. S.; Nimlos, M. R.; Brady, J. W.; Foust, T. D. *Science* **2007**, *315*, 804−807.

(6) Lynd, L. R.; Cruz, C. H. *Science* **2010**, *330*, 1176.

(7) Rehm, B. H. A. *Nat. Rev. Microbiol.* **2010**, *8*, 578−592.

(8) Szymanski, C. M.; Michael, F. S.; Jarrell, H. C.; Li, J.; Gilbert, M.; Larocque, S.; Vinogradov, E.; Brisson, J. R. *J. Biol. Chem.* **2003**, *278*, 24509−24520.

(9) Lamari, F. N.; Kuhn, R.; Karamanos, N. K. *J. Chromatogr., B: Anal. Technol. Biomed. Life Sci.* **2003**, *793*, 15−36.

(10) Dell, A. *Methods Enzymol.* **1990**, *193*, 647−660.

(11) Harvey, D. J. *J. Am. Soc. Mass Spectrom.* **2001**, *12*, 926−937.

(12) Adamson, J. T.; Hakansson, K. *Anal. Chem.* **2007**, *79*, 2901−2910.

(13) Xie, Y. M.; Lebrilla, C. B. *Anal. Chem.* **2003**, *75*, 1590−1598.

(14) Harvey, D. J.; Bateman, R. H.; Green, M. R. *J. Mass Spectrom.* **1997**, *32*, 167−187.

(15) Zhang, L.; Reilly, J. P. *J. Proteome Res.* **2009**, *8*, 734−742.

(16) Budnik, B. A.; Haselmann, K. F.; Elkin, Y. N.; Gorbach, V. I.; Zubarev, R. A. *Anal. Chem.* **2003**, *75*, 5994−6001.

(17) Zhao, C.; Xie, B.; Chan, S. Y.; Costello, C. E.; O'Connor, P. B. *J. Am. Soc. Mass Spectrom.* **2008**, *19*, 138−150.

(18) Wolff, J. J.; Amster, I. J.; Chi, L. L.; Linhardt, R. J. *J. Am. Soc. Mass Spectrom.* **2007**, *18*, 234−244.

(19) Kornacki, J. R.; Adamson, J. T.; Hakansson, K. *J. Am. Soc. Mass Spectrom.* **2012**, *23*, 2031−2042.

(20) Wolff, J. J.; Leach, F. E.; Laremore, T. N.; Kaplan, D. A.; Easterling, M. L.; Linhardt, R. J.; Amster, I. J. *Anal. Chem.* **2010**, *82*, 3460−3466.

(21) Han, L.; Costello, C. *J. Am. Soc. Mass Spectrom.* **2011**, *22*, 997−1013.

(22) Williams, J. P.; Grabenauer, M.; Holland, R. J.; Carpenter, C. J.; Wormald, M. R.; Giles, K.; Harvey, D. J.; Bateman, R. H.; Scrivens, J. H.; Bowers, M. T. *Int. J. Mass Spectrom.* **2010**, *298*, 119−127.

(23) Harvey, D. J.; Scarff, C. A.; Crispin, M.; Scanlan, C. N.; Bonomelli, C.; Scrivens, J. H. *J. Am. Soc. Mass Spectrom.* **2012**, *23*, 1955−1966.

(24) Isailovic, D.; Plasencia, M. D.; Gaye, M. M.; Stokes, S. T.; Kurulugama, R. T.; Pungpapong, V.; Zhang, M.; Kyselova, Z.; Goldman, R.; Mechref, Y.; Novotny, M. V.; Clemmer, D. E. *J. Proteome Res.* **2012**, *11*, 576−585.

(25) Wyttenbach, T.; Bleiholder, C.; Bowers, M. T. *Anal. Chem.* **2013**, *85*, 2191−2199.

(26) Edge, C.; Parekh, R.; Rademacher, T.; Wormald, M.; Dwek, R. *Nature* **1992**, *358*, 693−694.

(27) Wolfenden, R.; Yuan, Y. *J. Am. Chem. Soc.* **2008**, *130*, 7548−7549.

(28) Duan, J.; Kasper, D. L. *Glycobiology* **2011**, *21*, 401−409.

(29) Nyska, A.; Kohen, R. *Toxicol. Pathol.* **2002**, *30*, 620−650.

(30) Fialkow, L.; Wang, Y. C.; Downey, G. P. *Free Radical Biol. Med.* **2007**, *42*, 153−164.

(31) Valko, M.; Leibfritz, D.; Moncol, J.; Cronin, M. T. D.; Mazur, M.; Telser, J. *Int. J. Biochem. Cell Biol.* **2007**, *39*, 44−84.

(32) Hodyss, R.; Cox, H. A.; Beauchamp, J. L. *J. Am. Chem. Soc.* **2005**, *127*, 12436−12437.

(33) Lee, M.; Kang, M.; Moon, B.; Oh, H. B. *Analyst* **2009**, *134*, 1706−1712.

(34) Masterson, D. S.; Yin, H. Y.; Chacon, A.; Hachey, D. L.; Norris, J. L.; Porter, N. A. *J. Am. Chem. Soc.* **2004**, *126*, 720−721.

(35) Yin, H.; Chacon, A.; Porter, N. A.; Yin, H. Y.; Masterson, D. S. *J. Am. Soc. Mass Spectrom.* **2007**, *18*, 807−816.

(36) Sun, Q. Y.; Nelson, H.; Ly, T.; Stoltz, B. M.; Julian, R. R. *J. Proteome Res.* **2009**, *8*, 958−966.

(37) Harvey, D. J.; Dwek, R. A.; Rudd, P. M. In *Current protocols in protein science*; Coligan, J. E., et al. (Editorial Board); Wiley: New York, 2006; Chapter 12, Unit 12-7.

(38) Zhao, Y.; Truhlar, D. G. *Theor. Chem. Acc.* **2008**, *120*, 215−241.

(39) Boese, A. D.; Martin, J. M. L. *J. Chem. Phys.* **2004**, *121*, 3405−3416.

(40) Blanksby, S. J.; Ellison, G. B. *Acc. Chem. Res.* **2003**, *36*, 255−263.

(41) Domon, B.; Costello, C. E. *Glycoconjugate J.* **1988**, *5*, 397−409.

(42) Stubbs, J. M.; Marx, D. *Chem.—Eur. J.* **2005**, *11*, 2651−2659.

(43) Hunter, E. P. L.; Lias, S. G. *J. Phys. Chem. Ref. Data* **1998**, *27*, 413−656.

(44) Bomse, D. S.; Woodin, R. L.; Beauchamp, J. L. *J. Am. Chem. Soc.* **1979**, *101*, 5503−5512.

(45) Bereman, M. S.; Comins, D. L.; Muddiman, D. C. *Chem. Commun.* **2010**, *46*, 237−239.

(46) Yu, X.; Huang, Y.; Lin, C.; Costello, C. E. *Anal. Chem.* **2012**, *84*, 7487−7494.

(47) Lewandrowski, U.; Resemann, A.; Sickmann, A. *Anal. Chem.* **2005**, *77*, 3274−3283.

(48) Wuhrer, M.; Koeleman, C. A. M.; Hokke, C. H.; Deelder, A. M. *Rapid Commun. Mass Spectrom.* **2006**, *20*, 1747−1754.

(49) Wuhrer, M.; Deelder, A. M.; van der Burgt, Y. E. *Mass Spectrom. Rev.* **2011**, *30*, 664−680.

10692

dx.doi.org/10.1021/ja402810t | *J. Am. Chem. Soc.* 2013, 135, 10684−10692